

# Development of Multi-channel APD (Amplitude Probability Distribution) Measuring Apparatus

Ronte Sunao, Arakawa Satoru

[Summary]

Multi-channel Amplitude Probability Distribution (APD) measuring equipment has been developed to meet the demand to precisely measure statistically non-stationary wireless signals such as OFDM for using wireless frequencies effectively and efficiently, measuring digital noise, and sensing wireless signals, etc. This article describes the architecture and main characteristics of the 32000-channel synchronous APD apparatus, and its effectiveness for various APD measurements.

## 1 Introduction

Extensions of wireless communication services and Increases of wireless terminals have advanced making effective use of limited electromagnetic frequencies resources such as OFDM(Orthogonal Frequency Division Multiplex) communication systems using densely them for frequency, time, and associate amplitude axis.

A key point in understanding the behavior of these signals is how to measure them simultaneously and quantitatively on the frequency, time, and concomitant amplitude axes as a method of expressing these signals uniquely.

The target measurement signals are not only artificial electromagnetic signals used for various communications methods, but are also noise classified into natural, artificial, and internal noise, as well as statistically non-stationary signals, such as wireless signals carrying sensing information.

In particular, from the viewpoint of evaluating the target signal on the amplitude axis, the Amplitude Probability Distribution (APD) method is known to be effective for investigating the nature of changes in signal amplitude. APD is defined as the proportion of time that the instantaneous amplitude of the measurement target waveform exceeds the amplitude threshold value in the measurement period<sup>(1)</sup>. The amplitude time variation of the measured target signal is considered as a stochastic process with a time parameter, and then it is defined mathematically as the complimentary function of the APD function (cumulative probability dis-

tribution).

This APD measurement method has been standardized as one quantitative measure of electromagnetic waves, following 10 years of discussions of results by the CISPR (International Special Committee on Radio Interference) working group.

APD measurement has long been investigated as a method for statistical analysis of electromagnetic noise<sup>(3,4)</sup>. Moreover, APD measuring instruments have a long history, starting first with vacuum tube circuits, and then becoming digitized<sup>(5,6,7)</sup> and multi-channel<sup>(8)</sup> as technology progressed. There are three recent examples: measurement by offline processing using DSP technology after A/D conversion of the IF-band signal using the frequency conversion function of the radio frequency (RF) analog circuits of a spectrum analyzer (SPA) as an instrument for APD measurement of wireless signals<sup>(8)</sup>; development of a 5-channel real-time ADP measurement apparatus combined with a SPA<sup>(9)</sup>; and single-channel APD measurement targeting ultra-wide bandwidth (UWB) signals<sup>(10)</sup>.

Methods for measuring non-stationary signals are required for simultaneous monitoring of the three frequency, time, and corresponding amplitude axes. By developing from conventional SPAs using frequency sweep methods to frequency analysis using Fast Fourier Transformation (FFT), real-time measurement of frequency vs. time-varying characteristics has been improved, but we cannot yet guarantee that the capture rate is adequate for proper frequency characteristics of the signal on the axis.

After assuring the signal capture rate on this time axis, the APD measurement method was introduced for the amplitude axis and a wideband multichannel APD measurement instrument for multi-channel frequencies is needed as a future instrument for measuring non-stationary signals. We have already developed a 16000-channel APD measurement apparatus<sup>(11)</sup>. This article describes the development and effectiveness of a planned wider band 32000-channel APD measuring apparatus. Section 2 outlines the developed APD measuring apparatus supporting simultaneous multichannel measurement; section 3 describes its key features, scalable Resolution Bandwidth (RBW), and the variable number of channels measured in real time. The developed APD measuring apparatus with a signal capture rate for 32000 channels is useful for measuring non-stationary signals, etc.

## 2 Structure of Developed Apparatus

Figure 1 shows the external appearance of the developed APD measuring apparatus. This article describes simultaneous measurement of signals for the three frequency, time, and amplitude axes. Like the SPA when observing signal bands such as electromagnetic waves, multichannel APD measurement targets IF signals after frequency conversion.



Figure 1 32000-Channel Multichannel APD Apparatus

At electromagnetic wave measurement, if we assume APD measurement of an IF-band signal that has been frequency-converted from an antenna-selected signal, the measurement system from the antenna section to the APD measurement must be configured as a wideband distortion-free transmission system.

Figure 2 shows a functional block diagram for this equipment. Digital signal processing, which easily achieves linear phase characteristic, is used to assure linearity of the observed signal band waveform.

To assure linearity on the amplitude axis for the target measurement IF signal, it is converted to a digital signal using an A/D converter (ADC) with good quantization noise over a wide dynamic range. This apparatus uses a high-performance, 16-bit, 200 MSPS commercial ADC. The digitized IF signal center frequency is converted to the optimum frequency for the final-stage DSP and, after orthogonally transformed to an I/Q signal (by Quadrature Detector), and is decimated to lower-speed signals. The DSP system clock has good phase noise characteristics. The IF-band signal is also band-limited by a filter with good linear phase characteristics to avoid aliasing.

The RBW and type of band-control filtering are key elements determining the characteristics when monitoring signal behavior on the frequency axis.

Measurement of frequency characteristics using an SPA, etc., uses a Gaussian filter as a RBW. This apparatus measures APD characteristics on the frequency axis and also has a suitable filter-type setting function for observing the proprietary signal waveform according to the communications systems and evaluating the code error characteristics. It has a FIR-type digital filter designed to

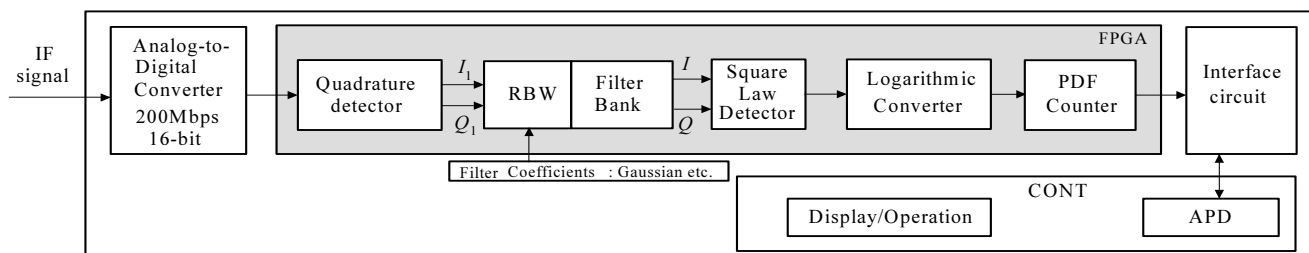


Figure 2 Block diagram of 32000-channel APD measuring apparatus

vary the filter characteristics by setting the linear phase impulse response coefficients at the filter multiplier (Filter coefficients in Fig.2). To support evaluation of characteristics for multi-carrier communications methods like OFDM, the Receiver (Rx) side measurement band must be wide and multi-channel. Having multichannels improves the measured frequency resolution at simultaneous measurement and is achieved using the filter-bank configuration.

Configuring a filter bank meeting the requirements for simultaneous measurement on the frequency and time axes, requires real-time measurement of the time signal with the frequency characteristics of each channel; in other words, it is necessary to assure the continuity of the time signal passing through each channel.

To achieve this filter bank, the short-time Fourier Transformation (FT) method shown in Eq. (1) expressed in a discrete-time system is adopted, which can change the number of channels flexibly and assures continuity to measure APD on the time axis.

From Eq. (2) derived from Eq. (1), the short-time FT method expresses the convolution sum (filtering) of the  $I$ ,  $Q$  time sequence signal  $x(n)$  and the impulse response  $v(-n)e^{-jn\omega} = v(-n)e^{-j\omega n}$  of a window-function RBW filter in Fig. 2 and frequency-converts the convolution result with the modulator, and converts it to the baseband signal.

In addition, when  $v(-n)$  of the frequency characteristics becomes  $V(e^{j\omega})$  the RBW impulse response frequency characteristics  $\hat{V}(e^{j\omega})$  become the filter shifted only by the frequency  $\omega_0$  as shown in Eq. (3). When there are  $M$  parts of this filter as  $m(=0, \dots, M-1)$ , a filter can be configured with  $M$  divisions distributed at each frequency  $m\omega_0$ . This calculation method allows the number of channels of the uniform filter bank to be changed easily.

$$X_{STFT}(e^{j\omega}, m) = \sum_{n=-\infty}^{\infty} x(n)v(n-m)e^{-j\omega n} \dots(1)$$

$$= e^{-j\omega m} \sum_{n=-\infty}^{\infty} x(n)v(n-m)e^{j\omega(m-n)} \dots(2)$$

$$\hat{V}(e^{-j\omega}) = \sum_{n=-\infty}^{\infty} v(-n)e^{-j(-\omega_0+\omega)n} = V(e^{-j(-\omega_0+\omega)}) \dots(3)$$

To understand the physical meaning of the above short-term FT, Eq. (1) becomes a method for multiplying the window function  $v(n-m)$  by the input signal series and calculating the discrete-time FT at every integer  $m$ . Using FFT to reduce the number of multiplication/addition processes in this discrete-time FT can configure a multichannel filter bank where RBW, the channel number and window function of which can be changed easily. With this development, we successfully configured the Rx bandwidth (RBW\*ch number = <32 MHz max.) with RBW ranging from 1 kHz to 1 MHz (1 to 3 steps), and also prepared 10 MHz (1 channel) and 20 MHz (1 channel).

“Continuity on the time axis” here means the number of time-series data necessary to execute meaningful APD measurement of the original time-varying amplitude; “The Sampling theorem on the time axis” means the number of sampled discrete data necessary to completely reproduce the original continuous signal.

The rules determining these conditions are standardized by CISPR16-1-1<sup>(2)</sup>; a sampling time of less than  $1/(10^6)$  per 10 seconds is recommended for a bandwidth of 1 MHz. Under the above conditions, looking from the viewpoint of the behavior of a signal composed of multiple sine waves in a band-limited width, irrespective of the size of the bandwidth, which has the same scalable linear structure as the one of another band-limited width, the sampling time can be based on a time that is at least 10 times the measurement bandwidth. This is the sample number required to faithfully obtain a time profile of the RBW band signal. This is the same as assuring the time-axis continuity for a configuration of multiple channels when each channel satisfies these conditions<sup>(12)</sup>.

After applying a Square Law Detector to the  $I$ ,  $Q$  time-series signal output of each channel and logarithmic conversion to the result, the contents of the counter addressed at each logarithmic value are referenced and incremented by +1 to reproduce a histogram using the PDF Counter equivalent to the Probability Distribution

Function at every 1 second.

Figure 2 shows the configuration of the above circuit. A Field Programmable Gate Array (FPGA) is used to construct the APD measurement circuit. After simulating the digital signal processing circuit and optimizing the number of multipliers and adders, memory storage and circuit resources, the circuit was synthesized in the FPGA. The operation word length required to assure the linearity on the digital signal processing amplitude axis adopted 30-bit fixed decimal point arithmetic to assure sufficient measurement level resolution for analysis at a RBW of 1 kHz.

The PDF value calculated for each channel is transferred via a high-speed bus interface (Interface Circuit) to the controller (CONT) to reproduce the APD values for the cumulative probability distribution using software.

This executes simultaneous and successive multichannel APD measurements allocated in the frequency interval equivalent to the RBW around any IF signal center frequency.

The measurement results are displayed as time versus amplitude using colored bands for each probability; the screen displays video results for APD versus amplitude using a Rayleigh<sup>(8)</sup> graph and amplitude versus APD using a semilogarithmic graph. The color-coded display is a powerful method for separating different signals with different probability densities. These measurement results are saved as necessary to a storage medium such as a hard disk. In designing the above software processing, we selected the controller CPU resources needed to achieve the real-time processing after analyzing the real-time processing for the configured modules.

From an installed system viewpoint, the APD measurement circuit data set by the operation section (Operation) is passed via the controller (CONT) interface and the channel number and RBW downloaded to the above-described FPGA are reproduced as the APD measurement equipment that can be reconfigured

scalably and flexibly.

For example, circuit data for a 1-kHz RBW filter with Gaussian characteristics and for short-term FT can be downloaded to the FPGA to achieve wideband APD measurement for up to 32734 channels at a measurement bandwidth of about 32 MHz.

Consequently, real-time and simultaneous multi-channel APD measurements are achieved and are furnished with a resolution of the RBW on the frequency axis, the required time resolution to execute APD measurement on the time axis, and linearity and high resolution on their attendant amplitude axis.

### 3 Main Characteristics for Multichannel Simultaneous APD Measurement

This section describes how to assure the filter-bank characteristics and signal capture rate for multichannel simultaneous measurement as well as its key features.

#### 3.1 Multichannel Filter Bank Separation Characteristics

Figure 3 shows the separation characteristics of the filter bank required to achieve multichannel simultaneous measurement with the frequency level characteristics results for each filter for 32000 channels. The filter bank frequency characteristics are shown when a CW signal is input as the IF signal and the RBW is set to 1 kHz. A uniform filter bank with Gaussian-type filters with a -3 dB bandwidth of 1 kHz is achieved, which are arranged in parallel every 1 kHz around 75.0 MHz as the center frequency.

Figure 3 shows the results for just 5 channels out of 32000 output channels positioned every 1 kHz. The frequency level values are instantaneous power averages calculated as expected random variables (amplitude) from PDF values. High measurement resolution is achieved on the frequency axis as a result of using the multichannel filter frequency separation characteristics, offering detailed time-frequency analysis for each channel.

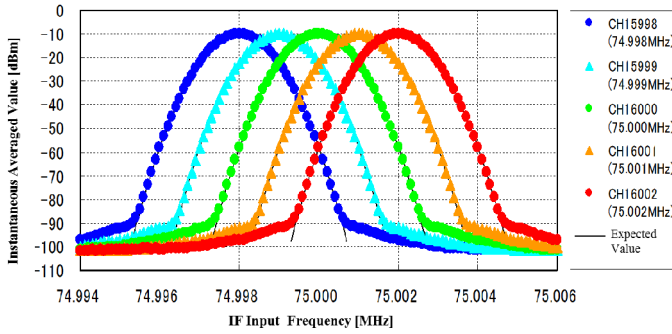


Figure 3 Frequency characteristics of 32000-ch filter bank

### 3.2 Securing Signal Capture Rate

Figure 4 shows a simple waveform for examining how to keep the signal capture rate above the 99% required for APD measurement, which is the only data to evaluate. The top part shows the relationship between actual measurement duration in the measurement period  $T_M$  and the measurement dead time  $T_X$  as the measurement dead time model.

The bottom part shows the pulse repetition frequency  $T_p$  and the time waveform for the instantaneous power of pulse width  $\tau_D$  as the pulse signal used for evaluation.

The maximum value of the APD for the pulse signal used for evaluation is  $APD \approx \tau_D / (T_M - T_X)$  when the pulse is fully within the measurement time. In addition, the time offset  $T_0$ , signifying the relative phase relationship between the pulse and dead time  $T_x$  increases by half the pulse width in each measurement period. When the pulse is completely within the dead time, it is set so APD becomes 0. When only part of the pulse is within the dead time, it is set so APD exceeds 0.

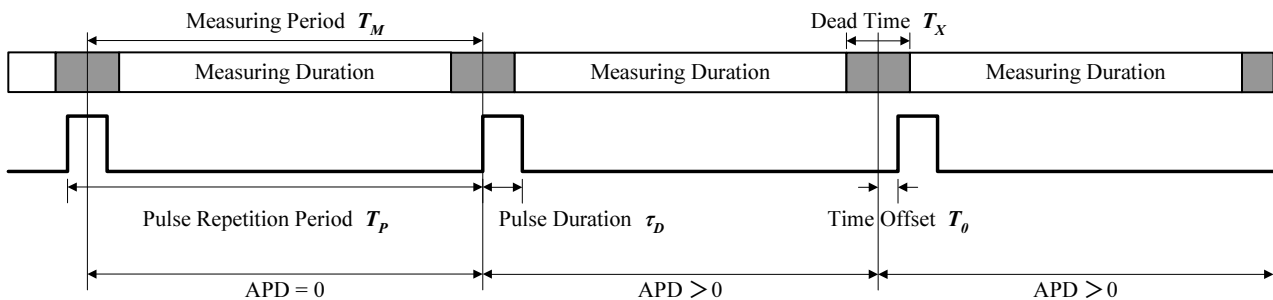


Figure 4 Evaluation waveforms for signal capturing rate

For the 1-second measurement period  $T_M$ , when measuring the APD for a pulse signal with a pulse repetition rate  $T_p$  of 1.005 s and a pulse width of  $\tau_D$  of 10 ms, if the APD measurement result is not 0, the signal dead time is within 1% and the signal capture rate is better than 99%. Figure 5 shows the signal capture rate measurement results when the RBW is 1 kHz and the number of measurement channels is 32000. The x-axis is time and the y-axis is APD[%].

Figure 5 indicates the APD is about 1% but there are 9 points where the APD is less than 1%. This shows the APD when part of the pulse is within some unknown dead time; there is no measurement with an APD value of 0 where the pulse is completely superimposed on the dead time. By applying this evaluation method, from the APD measurements for all RBS settings, it is clear the dead time is within 1% and the signal capture rate is better than 99%.

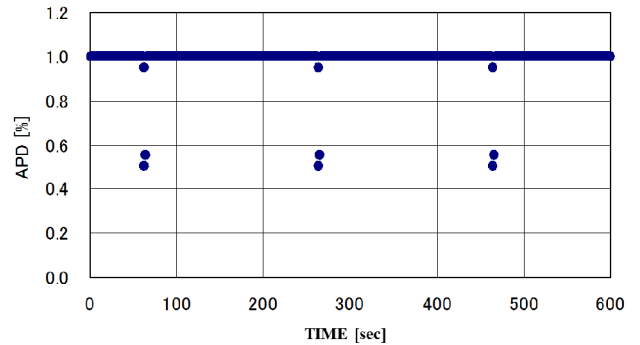


Figure 5 APD measured value for pulsed signals

### 3.3 Multichannel Real-Time APD Spectrum Waveform

Multichannel APD measurement functions as a wideband real-time APD spectrum analyzer by measuring multiple channels simultaneously. In addition, the amplitude probability distribution can be analyzed in detail for each channel. Figure 6 shows the simultaneous APD measurement results for RBW set to 1 kHz and 32000 channels when inputting five ISDB-T signals in parallel as IF input signals. The x-axis shows the channel arranged by frequency and the y-axis shows the instantaneous average power indicated by color bands according to probability. The screen is refreshed every 1 second and the APD value is indicated in real time every 1 second with no missed measurements, offering wideband (about 32 MHz), real-time APD measurements. The red color band indicates  $90\% < APD$ , yellow indicates  $50\% < APD \leq 90\%$ , green indicates  $10\% < APD \leq 50\%$ , light-blue indicates  $1\% < APD \leq 10\%$ , and blue indicates  $0\% < APD \leq 1\%$ . The correspondence between color bands and probability rates can be set as required.

For comparison with a conventional SPA, the same signal was input to an FFT SPA and the data captured every 1 second was analyzed by FFT; Figure 7 shows the detected averaged results. Comparing Figures 6 and 7, the multi-channel real-time APD measurement and color displays

provide a clearer understanding of the amplitude occurrence frequencies in the RBW band.

Figure 6 shows the signal components for the red spikes where the APD exceeds 90%. On the other hand, Figure 8 shows the APD measurement results for a signal when 5.6-MHz band AWGN (Additive White Gaussian Noise) occurs in 5 channels. Comparing Figures 6 and 8, the red signal spikes are clearly non-stationary Pilot signals characterizing ISDB-T signals.

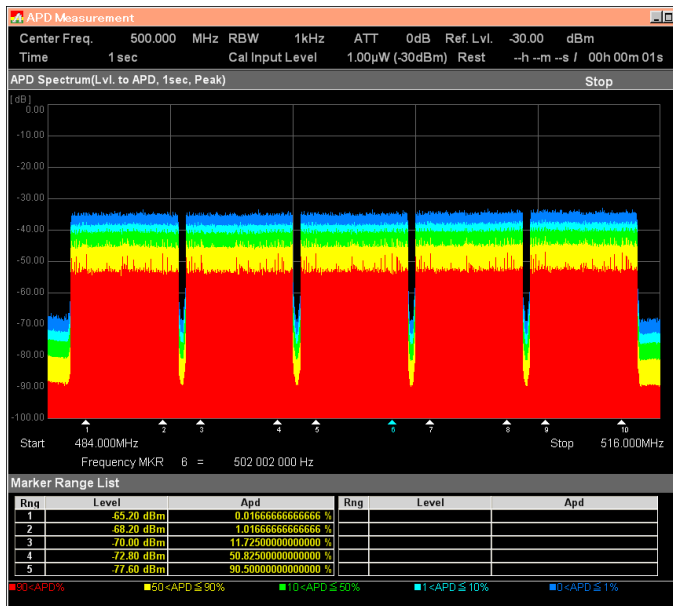


Figure 6 32000-ch APD Spectrum (5-ch ISDB-T signals)

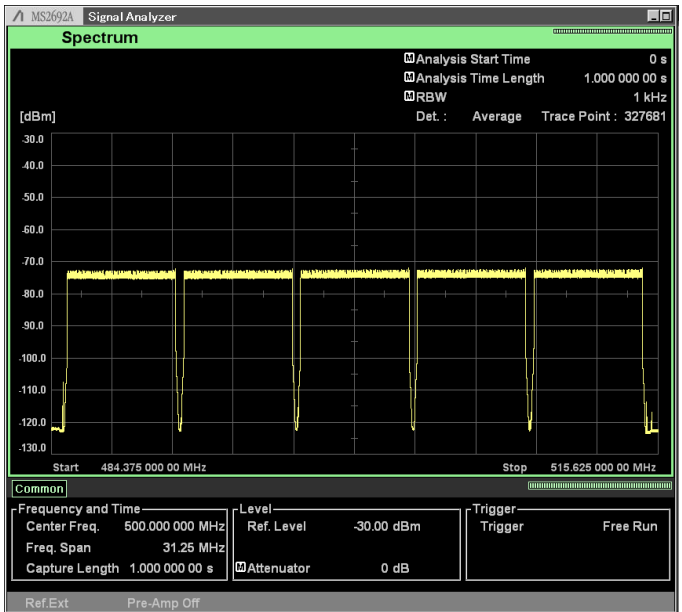


Figure 7 FFT Spectrum with averaged detection

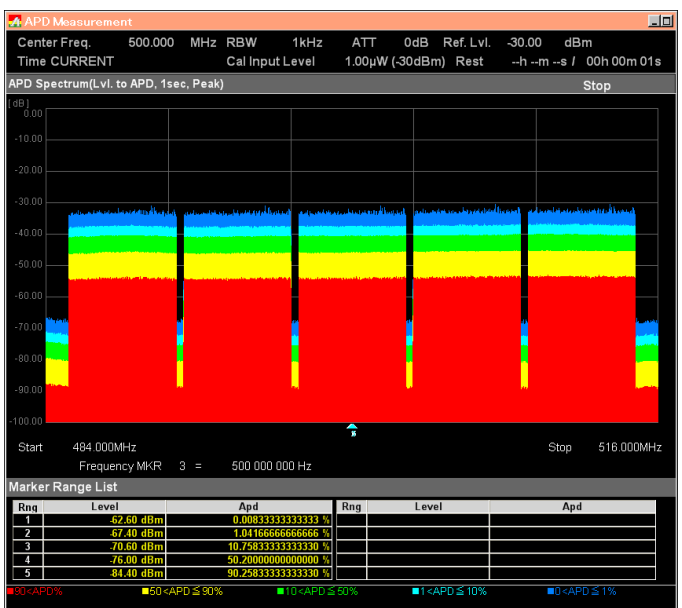


Figure 8 32000-ch APD Spectrum (AWGN signals)

### 3.4 Non-Stationary Signal Separation

Since multichannel APD is a wideband statistical APD measurement method, signals with different statistical distributions can be separated.

Figure 9 shows the measurement results when the RBW is set to 1 kHz and the number of channels is set to 16000 and two signals with different probability distributions are input as IF signals; the signals are pulse repetition modulation signals with the Gaussian noise shown in Table 1.

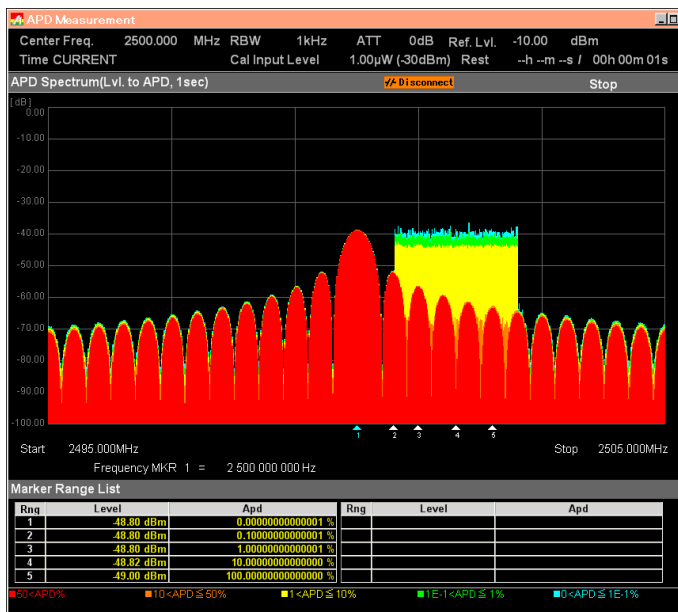


Figure 9 16000-ch APD Spectrum

Table 1 Specification of measurement signals

Pulse modulation Signal: Carrier frequency: 2.5 GHz Pulse Repetition Frequency: 125/Pulse Width: 2.5 μs Output Level: -15 dBm
Gaussian Noise Signal: Center Frequency: 2.5016 GHz, Bandwidth: 2 MHz Duration Time/Generation Cycle: 100 ms/1 s Output Level: -25 dBm

For comparison, Figure 10 shows the measurement results analyzed by an FFT SPA when capturing the same input signals every 1 second with the frequency span set to 10 MHz and the RBW set to 1 kHz. From Figures 9 and 10, the FFT analysis results using a conventional SPA do not clearly separate the two signals, whereas the multichannel APD measurement does separate them. This result is due to the real-time measurement of the multichannel APD

measurement method and the color display of the probability distribution. Additionally, the APD display results in Figure 9 are refreshed every 1 second, whereas the FFT analysis requires about 4 minutes of processing time until signals captured each second can be displayed.

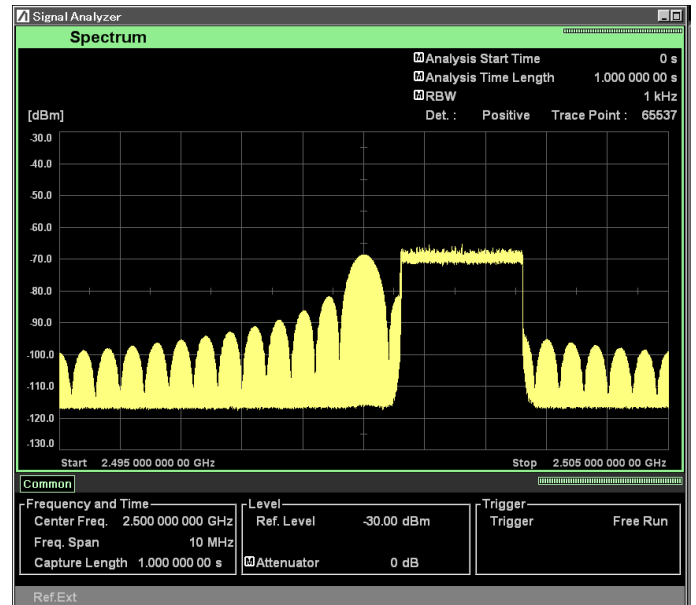


Figure 10 FFT Spectrum with peakhold detection

### 3.5 Amplitude Probability Distribution Measurement

Multichannel APD measurement with RBW set to 1 kHz can display the statistical nature of each measured signal channel using intuitive, accurate, and real-time display of the measurement results.

Figure 11 shows the results for 5-channel APD measurement of internal floor noise of the developed apparatus with the IF input terminated at 50 Ω pure resistance with the frequency ranging from 74.998 to 75.002MHz and a RBW of 1kHz. The x-axis shows the probability as a Rayleigh measure<sup>(3)</sup>, and the y-axis shows the amplitude level. These graphs are called the APD curve.

In this measurement example, the linearity indicating the distribution and the gradient can be used as an estimate of the thermal noise. In this case, the statistical nature of the characteristics can be easily understood because the statistical distribution can be measured in real time.

In addition, it is also possible to investigate the noise band characteristics. Since the multichannel APD measurement function is scalable with changeable settings for

the RBW and number of channels, it is possible to evaluate band characteristics by measuring noise for each RBW<sup>(11)</sup>.

The top part of Figure 11 is a graphical expression of the APD curve while the lower part quantifies the power, peak power, and PAPR (Peak to Average Power Ratio) for each channel as concrete values in real time.



Figure 11 32000-ch APD Spectrum (floor noise)

### 3.6 Supporting EMC Measurement

Since multichannel APD measurement performs frequency-time analysis with a guaranteed signal capture rate of better than 99%, it can be used for noise measurements requiring instantaneous measurement.

In fact, the CISPR standards body is currently investigating APD measurement and the permissible values as a substitute method for the microwave noise compliance test.

Since the RBW and channel settings for this apparatus are scalable, it offers a measurement environment matching the requirements of the Japanese CISPR/B/WG1 APD maintenance team currently investigating standards and performing tests. Their results are reported in reference 14. Microwave noise measurements require measurement of the reference frequency (near 2.4 GHz) and measurements up to the 4th-order harmonic. These noise waveforms are characterized by frequency changes over time and have required simultaneous measurement of 11 channels at 5 MHz on both sides of the center frequency with RBW set to 1

MHz. In comparison to these settings, the multichannel APD measurement apparatus supports 16 channels with an RBW setting of 1 MHz.

The measurement up to the 4th-order harmonic uses a newly developed tunable preselector up to 26.5 GHz with conversion to a 75 MHz IF signal and APD measurement of that band signal.

Figure 12 shows the APD curve of 10 channels for 10 minutes, measuring the 2nd-order harmonic radiated from the microwave. The y-axis indicates the probability and the x-axis the amplitude threshold level. It shows the probability versus level. Simultaneous display of APD values for 10 channels provides an intuitive grasp of the changes between channels in the 10-MHz band. In addition, since the appearance frequency of the signal amplitude threshold level is an important index when planning permissible values, this apparatus has marker functions for setting markers on the x and y-axes. The numerical measurement results at the marker positions are indicated below the APD curve.

Figure 13 shows the APD chart for 10 minutes for 5 channels to help understand the shift in the APD measurements over time. The change in the APD value every 1 second is displayed to indicate the measured signal time variation and characteristics such as the periodicity. This can be used to estimate the measurement time required to clarify the measurement target phenomena.

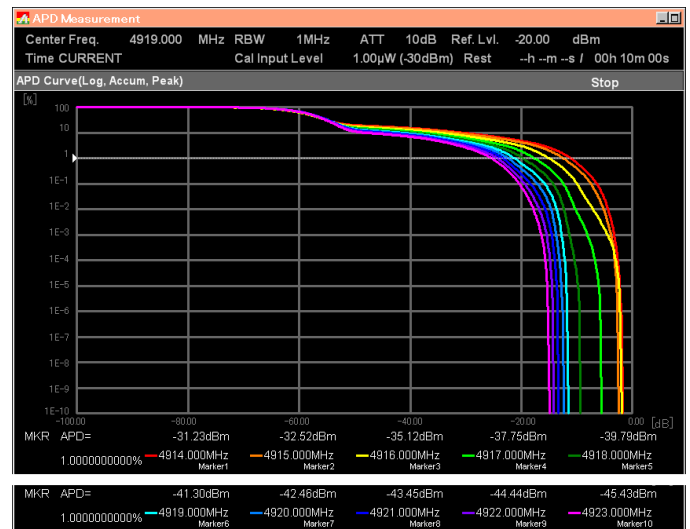


Figure12 APD Curve (4914 to 4923 MHz)



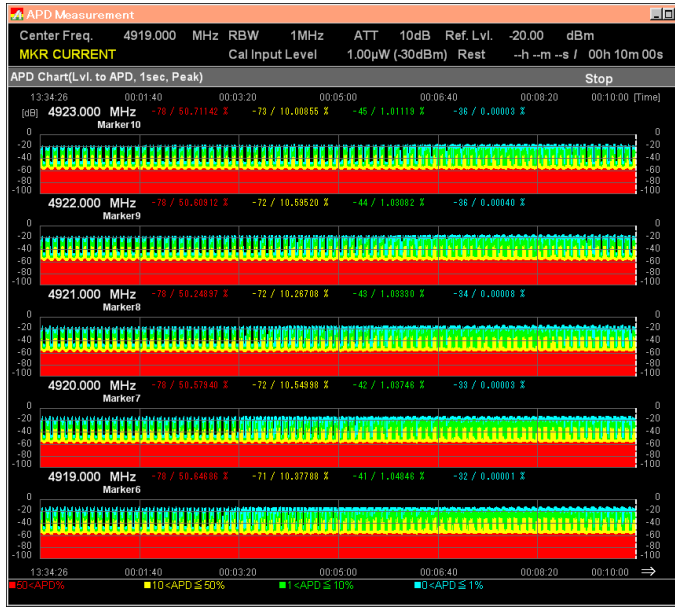


Figure 13 APD Chart (4919 to 4923 MHz)

### 3.7 RF Modulation Pulse Wave Measurement

Since multichannel APD measurement is a real-time measurement method with an assured signal capture rate of better than 99% as described in section 3.2, it can be used to measure the peak values of impulse-type noise and to understand electromagnetic phenomena with a low occurrence probability of less than  $10^{-9}$  (at 1 MHz RBW)<sup>(9)</sup>.

Figure 14 shows the measurement results for a pulse modulation RF signal with a carrier frequency of 75 MHz, a pulse repetition cycle of 1 s, a pulse width of 10 ms, and a pulse height of 0 dBm. The RBW is a -3 dB Gaussian filter set to 1 kHz.

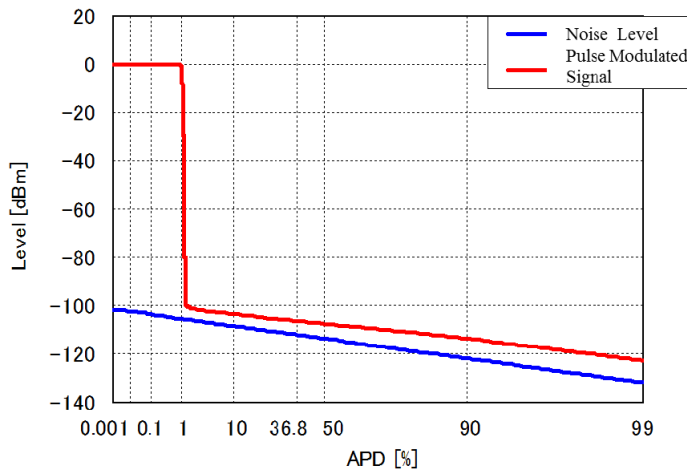


Figure 14 APD Curve of RF modulated pulse signal

The pulse wave occurrence probability calculated from the pulse repetition cycle and pulse width is accurately matched to the measured value of 1% in Figure 14.

### 3.8 APD Features and Support for Wireless Communications

The amplitude probability distribution differs according to the modulation method used by the wireless communications. These characteristics can be captured efficiently by APD measurements to identify the type of modulation<sup>(15)</sup>. Figure 15 shows the APD measurement results for one channel measured using the Anritsu MS2690A1 5 channel APD measuring instrument, opening the possibility for modulation identification applications.

When used for this type of characterization, it may be possible to detect jamming phenomenon from differences in APD characteristics with and without jamming at waveform monitoring<sup>(16)</sup>.

Additionally, there are reports on the correlation between interference and coding error rates in wireless communications, and applications in error rate measurements are anticipated<sup>(17)</sup>.

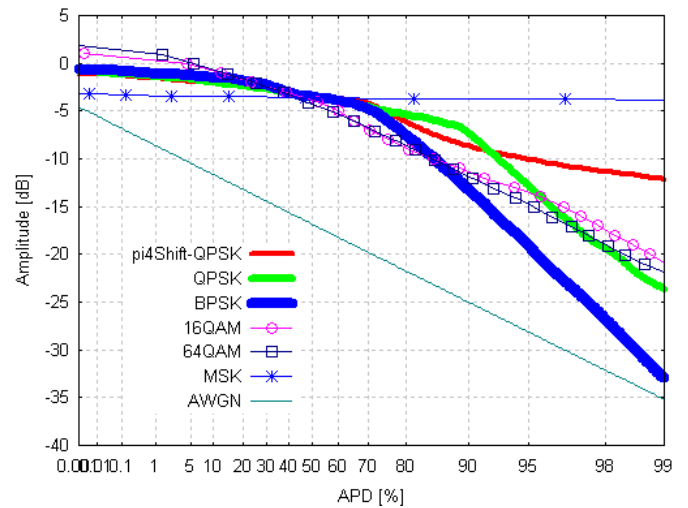


Figure 15 APD Curve versus modulation systems<sup>(10)</sup>

## 4 Summary

We have described development of a multichannel APD measuring apparatus that is expected to offer an efficient method for measuring the increasingly complex wireless environment, helping make more efficient use of the wireless frequency spectrum. Multichannel APD measurement assures a signal capture rate of better than 99% for time-frequency analysis and can be used to examine amplitude data in real time. It is expected to have useful future applications in a diverse range of wireless frequency environments such as cognitive wireless communications, wireless interfaces in smart grids, remote control of robots by wireless communications, etc.

Part of this research was supported by the Ministry of Internal Affairs and Communications project on Research and Development of the Utilization of Electric Wave Resources.

## References

- 1) Y. Shimizu, A. Sugiura, "Fundamentals and Countermeasures for electromagnetic interference", IEICE edition, CORONA PUB. (1995), in Japanese.
- 2) CISPR16-1-1 2nd ed., "Specification for Radio Disturbance and Immunity Measuring Apparatus and Methods" (2006)
- 3) H. Yuhara, T. Ishida, and M. Higashimura, "Measurement of the Amplitude Probability Distribution of Atmospheric Noise", Journal of the Radio Research Laboratories, Vol.3, pp.101-108 (1956-2)
- 4) M. Kanda, "Time and Amplitude Statistics for Electromagnetic Noise in Mines", IEEE Trans. on Electromagnetic Compatibility, Vol.EMC-17, No.3, pp.122-129 (1975-8)
- 5) M. Uchino, T. Shinozuka, and R. Sato, "Amplitude probability distribution measuring equipment with 20-MHz sampling and 8-bit resolution", Electronics and communications in Japan, Part I, Vol. 84, No. 2, pp. 1-7, (2001-2), in Japanese.
- 6) M. Uchino, M. Hitsuyama, T. Shinozuka, and Y. Kami, "Radio Noise Analyzer having Multi-Channel Amplitude Probability Distribution Measuring Function", Proceedings of the 2009 IEICE General Conference, B-4-75,p.418,(2009-03), in Japanese.
- 7) M. Uchino, O. Tagiri, and T. Shinozuka, "Real-Time Measurement of Noise Statistics", IEEE Trans. Electromagnetic Compatibility, Vol.43, No.4, pp.629-636 (2001-11)
- 8) K. Gotoh, Y. Matsumoto, S. Ishigami, T. Shinozuka, and M. Uchino, "Development and evaluation of a prototype multi-channel APD measuring receiver", 2007 IEEE International Electromagnetic Compatibility Symposium, THPM6SS2, Hawaii (2007-7)
- 9) S. Arakawa, S. Ronte, T. Otsuka, H. Aso, and M. Uchino, "Continuous Measurement of Amplitude Probability Distribution and Applications to Pulses of Low Occurrence Frequency", IEEEJ Transactions on FM, Vol.129, No.8, (2009-1), in Japanese.
- 10) K. Mochizuki, Y. Kimura, H. Watanabe, and M. Uchino, "Peak power measurement of UWB transmissions using 50-MHz bandwidth gaussian filter", 'Proceedings of Asia-Pacific Microwave Conference 2010, Yokohama, December 8-10, 2010.
- 11) S. Ronte, S. Arakawa, T. Otsuka, and M. Uchino, "Development of 16000 channel Amplitude Probability Distribution measuring equipment and its evaluation of Quantized noise measurement", The 27<sup>th</sup> Sensing Forum, SICE, pp107-111,(2010-9), in Japanese.
- 12) S. Ronte, S. Arakawa, T.Otsuka, and M. Uchino, "Development of 32000 channel Amplitude Probability Distribution Measuring Equipment", The 55<sup>th</sup> Annual Conference of the Institute of Systems, Control and Information Engineers, T27-5, CD-ROM (2011-5), in Japanese.
- 13) M. Shinji, et al, "Radio-wave propagation of radio communication", IEICE edition, CORONA PUB.(1992), in Japanese.
- 14) S. Gotoh, CISPR/B/WG1/APD(Shinozuka,Gotoh)/11-03,2011-2
- 15) R. Tokubo, H. Hosoya, S. Ronte, and M. Uchino, "Classification of Modulation by Using Amplitude Probability Distribution", Proceedings of the 2010 IEICE General Conference, B-5-15, p.447, (2010-03), in Japanese.
- 16) H. Hosoya, R. Tokubo, S. Ronte, and M. Uchino, "A detection of Interferences by Using Amplitude Probability Distribution", Proceedings of the 2010 IEICE General Conference, B-5-16,p.448,(2010-03), in Japanese.
- 17) Y. Matsumoto, "On the relation Between the Amplitude probability Distribution of Noise and Bit error Probability", IEEE Transactions on Electromagnetic Compatibility, VOL.49, NO.4, pp.940-941(2007-10)

---

## Authors



**Ronte Sunao**  
1st Technology Development Dep.  
R&D Center.  
R&D Div.



**Arakawa Satoru**  
Project Team 1.  
Product Marketing Dep.  
Marketing Div.

Publicly available